MEDICAL SCIENCE MONITOR

ANIMAL STUDY

e-ISSN 1643-3750
© Med Sci Monit, 2020; 26: e921580
DOI: 10.12659/MSM.921580

Received: 2019.11.21
Accepted: 2020.01.27
Available online: 2020.02.06
Published: 2020.02.12

Integrative Analysis of Long Non-Coding RNAs (lncRNAs), miRNAs, and mRNA-Associated ceRNA Network in Lung Tissue of Aging Mice and Changes After Treatment with *Codonopsis pilosula*

Authors' Contribution:
Study Design A
Data Collection B
Statistical Analysis C
Data Interpretation D
Manuscript Preparation E
Literature Search F
Funds Collection G

CDE 1 Dongmei Chen
B 1 Jiajia Liu
F 1 Jie Meng
B 1 Dandan Li
F 1 Pan Zhao
D 2 Yongqiang Duan
AEG 1,3 Jing Wang

1 School of Clinical Medicine, Gansu University of Chinese Medicine, Lanzhou, Gansu, P.R. China
2 School of Basic Medicine, Gansu University of Chinese Medicine, Lanzhou, Gansu, P.R. China
3 The Key Laboratory of Traditional Chinese Herbs and Prescription Innovation and Transformation of Gansu Province, Gansu University of Chinese Medicine, Lanzhou, Gansu, P.R. China

Corresponding Author: Jing Wang, e-mail: jwang_2017@hotmail.com
Source of support: This research was funded by the National Natural Science Foundation of China (grant number 81760835) and the General Project of Scientific Research in Colleges and Universities of Gansu Province (grant number 2018A-052)

Background: *Codonopsis pilosula* is a traditional Chinese medicine that has an anti-aging effect. However, the anti-aging effect of *Codonopsis pilosula* on the lungs remains largely unknown, and the molecular mechanism also needs to be further studied. Thus, we investigated the protective effect of *Codonopsis pilosula* on the lungs of aging mice, and explored the underlying molecular mechanism.

Material/Methods: We established an aging mouse model and then treated the mice with *Codonopsis pilosula*. Microarray analysis and bioinformatics methods were used to comprehensively analyze the lncRNA-miRNA-mRNA (ceRNA) network.

Results: Our results showed that we successfully established the aging mouse model. The microarray analysis showed that 138 lncRNAs, 128 mRNAs, and 7 miRNAs were significantly changed after aging, and 282 lncRNAs, 283 mRNAs, and 19 miRNAs were dysregulated after treatment with *Codonopsis pilosula*. To explore the signaling pathways involved, KEGG pathway analysis was performed. Compared with the ceRNA network in aging mice and after treatment with *Codonopsis pilosula*, we found that 3 mRNAs (Hif3a, Zbtb16, Plxna2) and 1 lncRNA (NONMMUT063872) were associated with the anti-aging effect of *Codonopsis pilosula* and they were validated by quantitative real-time polymerase chain reaction (qRT-PCR) analysis.

Conclusions: Our results showed that *Codonopsis pilosula* has a protective effect on the aging lung, and the ceRNA network plays an important role in the anti-aging effect of *Codonopsis pilosula*.

MeSH Keywords: Aging • Codonopsis • Lung Diseases • Microarray Analysis

Full-text PDF: https://www.medscimonit.com/abstract/index/idArt/921580

Indexed in: [Current Contents/Clinical Medicine] [SCI Expanded] [ISI Alerting System] [ISI Journals Master List] [Index Medicus/MEDLINE] [EMBASE/Excerpta Medica] [Chemical Abstracts/CAS]

Background

Aging is a complicated process that affects most body systems, leading to a gradual loss of function [1]. With the increased aging of the global population, problems associated with aging are attracting greater attention [2]. Aging can cause changes in lung structure and function, leading to various lung diseases [3]. The incidence and mortality rates of chronic and acute lung diseases increase with age [4]; therefore, effective strategies for the treatment and prevention of age-related lung diseases are essential for prolonging life and maintaining health. *Codonopsis pilosula* is a perennial herbaceous plant that mainly grows in East Asia, Southeast Asia, and Central Asia [5]. It has been used as a traditional Chinese medicine since ancient times, with the effect of invigorating the spleen and tonifying the lung, as well as tonifying blood and invigorating Jin [5]. Studies indicated that *Codonopsis pilosula* has an anti-aging effect [6,7], but the anti-aging effect of *Codonopsis pilosula* on the lungs remains largely unknown, and previous studies have mainly concentrated on the post-transcriptional and epigenetic levels. Therefore, the molecular mechanism underlying the anti-aging effect of *Codonopsis pilosula* needs to be further studied.

Traditional Chinese medicine, using complex compositions, acts through multiple targets and levels; therefore, it is necessary to use the systems biology approach to study the network as a whole. Pandolfi et al. [8] were the first to propose the ceRNA hypothesis, suggesting that different types of RNA molecules compete to bind to miRNA, thus reducing the inhibitory effect of miRNA on their mRNA targets. Based on the ceRNA theory, many scholars have studied the role of ceRNA networks in various diseases [9–11]. Many studies have indicated that ceRNA networks play important roles in biological processes [9–11]. However, there has been no published research on the role of the ceRNA network in the anti-aging effect of *Codonopsis pilosula*, and this warrants further study.

Thus, to investigate the protective effect of *Codonopsis pilosula* on the lungs of aging mice, *Codonopsis pilosula* water extract was used to treat the aging model mice, and we assessed the biochemical, pathological, and ultrastructural changes in lung tissue. To study the molecular mechanism involved, microarray analysis and bioinformatics methods were used to comprehensively analyze changes in the ceRNA network in aging mice after treatment with *Codonopsis pilosula*, which is the theoretical basis for the anti-aging effect of *Codonopsis pilosula*.

Material and Methods

Animals

One hundred SPF-grade Kunming mice (50 females and 50 males) were purchased from the Scientific Experimental Animal Center of Gansu University of Chinese Medicine, animal production certificate number: SCXK (gan) 2015-0002. Mice were 2 months old, with an average body weight of 20±2 g. They were raised at the Scientific Experimental Animal Center of Gansu University of Chinese Medicine (temperature 20~25°C, free access to drinking water and feeding, and natural light), certificate number: SCXK (gan) 2015-0005. All experimental procedures and protocols were performed according to the guidelines of the Institutional Animal Ethics Committee of Gansu University of Chinese Medicine (No. 2017-106).

Drug preparation and reagents

Identified white *Codonopsis pilosula* was used in this experiment. We boiled 100 g *Codonopsis pilosula* twice in water, for 1 h each time. The double-extracted solutions were combined, filtered, and concentrated into a water decoction containing 0.5 g·mL^{-1} original medicinal material, then it was placed in a refrigerator (4°C) until later use. The water decoction was prepared fresh every 5 days. D-galactose was purchased from Sigma (USA), and 12 g·L^{-1} was prepared with normal saline before use. Superoxide dismutase (SOD) kits were purchased from Nanjing Jiancheng Bioengineering Research Institute (Nanjing, China).

Mouse model

All mice were randomly divided into a control group, a model group, and low- (LC), middle- (MC), and high-dose *Codonopsis pilosula* treatment (HC) groups. Each group contained 20 mice (10 males and 10 females). D-galactose solution (50 g·L^{-1}) was injected subcutaneously into the neck and back of the model, LC, MC, and HC groups, with the injection volume of 0.025 mL·g^{-1}. The control group was given the same amount of normal saline. On the 11th day of modeling, the *Codonopsis pilosula* treatment groups were administered 5, 10, or 15 g·kg^{-1} of *Codonopsis pilosula* every morning through intragastric administration. The control group and the model group were given the same amount of normal saline as the *Codonopsis pilosula* treatment groups. Continuous modeling was performed for 42 days.

Determination of SOD activity, lung weight, and lung organ coefficient

After modeling, we took blood samples to determine serum SOD activity following the kit instructions. All mice were

Indexed in: [Current Contents/Clinical Medicine] [SCI Expanded] [ISI Alerting System] [ISI Journals Master List] [Index Medicus/MEDLINE] [EMBASE/Excerpta Medica] [Chemical Abstracts/CAS]

weighed and then sacrificed according to a standard protocol and were dissected by professional pathologists. We completely removed the lungs, carefully removed the fat and connective tissue around the lungs, and used filter paper to absorb the blood and body fluid from the surface of the lungs. Body weight was measured in the normal living body, and the lung weight was measured and recorded by the routine method. We calculated the organ coefficient after weighing the organs as follows: Organ coefficient (%)=organ weight (g)/body weight (g)×100%.

Hematoxylin-eosin staining

To observe the pathological and morphological changes in lung tissue in each group of mice, we performed hematoxylin-eosin staining. The lungs were cut and soaked in 4% paraformaldehyde solution after being rinsed with normal saline and dried with filter paper. The lungs were then fixed at room temperature, embedded in paraffin, and cut into 3-μm slices. After dewaxing and washing, we performed hematoxylin-eosin staining and observed the slices under a microscope after sealing.

Transmission electron microscopy

To observe the ultrastructural changes of lung tissue cells in the control group, the model group, and HC group, we performed transmission electron microscopy. We cut the lungs into about 1-mm^3 pieces after rinsing and drying, and then we placed them in a pre-cooled 2.5% glutaraldehyde solution at 4°C to fix overnight. After rinsing 3 times with PBS, 1% osmic acid staining, dehydration, soaking, embedding, and polymerization, we cut the lungs into 70-nm sheets, re-dyed them, and then performed transmission electron microscopy.

RNA extraction, labeling, and hybridization

Total RNA containing small RNA was extracted from lung tissues in the control group, model group, and HC group (n=3 mice) using Trizol reagent (Invitrogen) and purified using a mirVana miRNA separation kit (Ambion, Austin, TX, USA). A spectrophotometer (NanoDrop ND-1000) was used to measure RNA purity and concentration at OD260/280. The integrity of RNA was determined by 1% formaldehyde denaturing gel electrophoresis. We used CapitalBio Technology Mouse LncRNA Array v1 (4×180K format) and the Agilent Mouse miRNA Microarray, Release 21.0 (8×60K format). Microarray experiments, including labeling and hybridization, were conducted according to the manufacturer's instructions.

Microarray data analysis

GeneSpring software V13.0 (Agilent) was used to analyze the lncRNA, mRNA, and miRNA array data for data summarization, normalization, and quality control. To select the differentially expressed genes, we used threshold values of ≥2 and ≤-2-fold change and a Benjamini-Hochberg corrected P value of 0.05. Through the Adjust Data function of CLUSTER 3.0 software, data were Log2 transformed and median-centered by genes. Finally, tree visualization was performed using Java Treeview (Stanford University School of Medicine, Stanford, CA, USA). Total RNA containing small RNA microarray data were uploaded to the GEO database (*http://www.ncbi.nlm.nih.gov/geo/*), accession number: GSE139876.

Function enrichment analysis

To study the biological function of differentially expressed mRNAs, KOBAS (KEGG Orthology Based Annotation System) was used to perform Gene Ontology (GO) enrichment analysis and Kyoto Encyclopedia of Genes and Genomes (KEGG) pathway enrichment analysis. GO enrichment analysis includes biological process (BP), cellular component (CC), and molecular function (MF). GO term and KEGG pathways were considered significantly enriched with P value <0.05.

Construction of ceRNA network in aging mice and after treatment with *Codonopsis pilosula*

The ceRNA network was constructed based on the theory that lncRNAs can affect miRNA and act as miRNA sponges to further regulate mRNA. In this study, lncRNA-miRNA target interaction was predicted by TargetScan local version. The miRNA-mRNA pairs were analyzed by TargetScan (*http://www.targetscan.org/index.html*). To construct the ceRNA network, we also calculated the pairwise Pearson correlation coefficients between lncRNA and miRNA, as well as miRNA and mRNA based on their expression levels. Only the pairs with $|r| > 0.8$ and $P<0.05$ were considered as co-expression in the model group compared with the control group and $|r| > 0.95$ and $P<0.05$ in the HC group compared with the model group. Negative lncRNA-miRNA and miRNA-mRNA co-expression pairs were identified with $r<0$. Thereby, lncRNA and mRNA regulated by the same miRNA were filtered out. The ceRNA network was constructed based on the lncRNA-miRNA network and miRNA-mRNA network. The ceRNA network was constructed as shown in Figure 1. Finally, these networks were constructed and visualized by Cytoscape 3.6.1.

Quantitative real-time polymerase chain reaction (qRT-PCR)

Total RNA was extracted from lung tissues of the control group, model group, and HC group (n=3 mice) using Trizol reagent [12] and quantified by spectrophotometer or Qubit, and its integrity was assessed by agarose gel electrophoresis or Agilent 2100. The quantitative detection of total RNA was carried out by

Indexed in: [Current Contents/Clinical Medicine] [SCI Expanded] [ISI Alerting System] [ISI Journals Master List] [Index Medicus/MEDLINE] [EMBASE/Excerpta Medica] [Chemical Abstracts/CAS]

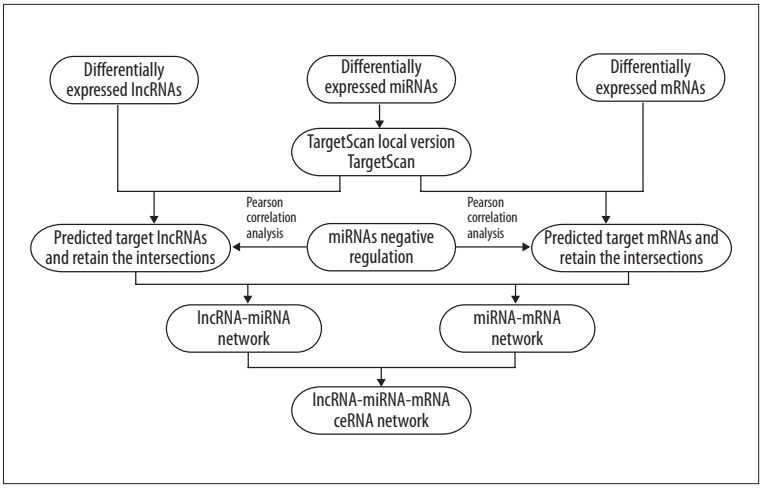

Figure 1. Flow chart of ceRNA network construction.

Table 1. PCR primers used in this study.

Name	Sequence
GAPDH	F GTTGTCTCCTGCGACTTCA R TGGTCCAGGGTTTCTTACTC
NONMMUT063872	F TTGGCACCAACTAGGAAGCAA R CACGAGGGATGGGACTTTGAA
Hif3a	F CTCGCCGTTTCTGTAGTCCA R CGGAAGAGGACTTTGGGGTC
Plxna2	F AGCTAAGAGCCCTGAATCCTCG R CTAGGTCCCTGAAGCCACTTTG
Zbtb16	F GGGAGGACCAGTGTCCCTTA R ACCATGCCCCAAGACCAAAA

SYBR green fluorescent dye method. Generally, random primers were used for reverse transcription, and the reverse cDNA template was assessed by quantitative PCR under the initiation of upstream and downstream primers. The primers used in this study are listed in Table 1. All lncRNA and mRNA expression data were normalized to GAPDH. The $2^{-\Delta\Delta Ct}$ method was used to calculate relative expression of genes.

Statistical analysis

Statistical analysis was performed using SPSS 24.0 statistical software. The experimental data are expressed as mean±standard deviation, and single-factor analysis of variance (ANOVA) was used for comparisons among multiple groups. $P<0.05$ was considered a significant difference between 2 groups.

Results

Determination of SOD activity, lung weight, and lung organ coefficient

In this study, the SOD activity of the model group was significantly decreased compared with the control group, but the SOD activity of the LC, MC, and HC groups was increased compared with the model group, and the SOD activity of the MC group and HC group was significantly increased (Figure 2A). The lung weights and lung organ coefficients of the model group were significantly decreased compared with the control group, but the lung weights and lung organ coefficients of the LC, MC, and HC groups were significantly increased compared with the model group (Figure 2B, 2C). These results showed that we successfully established the aging model, and *Codonopsis pilosula* had a protective effect on the lungs of aging mice.

Morphological observation of lung tissue

The control group had clear alveolar structure and uniform alveolar septum thickness (Figure 3A). In the model group, the alveolar septum was widened, fibroblasts were proliferated, and many extracellular matrixes were gathered together (Figure 3B). In the LC group, the thickness of some alveolar septa was uneven, and the accumulation of extracellular matrix could be seen (Figure 3C). In the MC group, the alveolar structure was relatively clear, the local alveolar septum was widened, and a small amount of extracellular matrix accumulation could be seen (Figure 3D). In the HC group, the alveolar structure was clear, the alveolar septum was uniform, and the structure was basically normal (Figure 3E). These results suggested that *Codonopsis pilosula* improved the pathology of lung tissue in aging mice.

Indexed in: [Current Contents/Clinical Medicine] [SCI Expanded] [ISI Alerting System] [ISI Journals Master List] [Index Medicus/MEDLINE] [EMBASE/Excerpta Medica] [Chemical Abstracts/CAS]

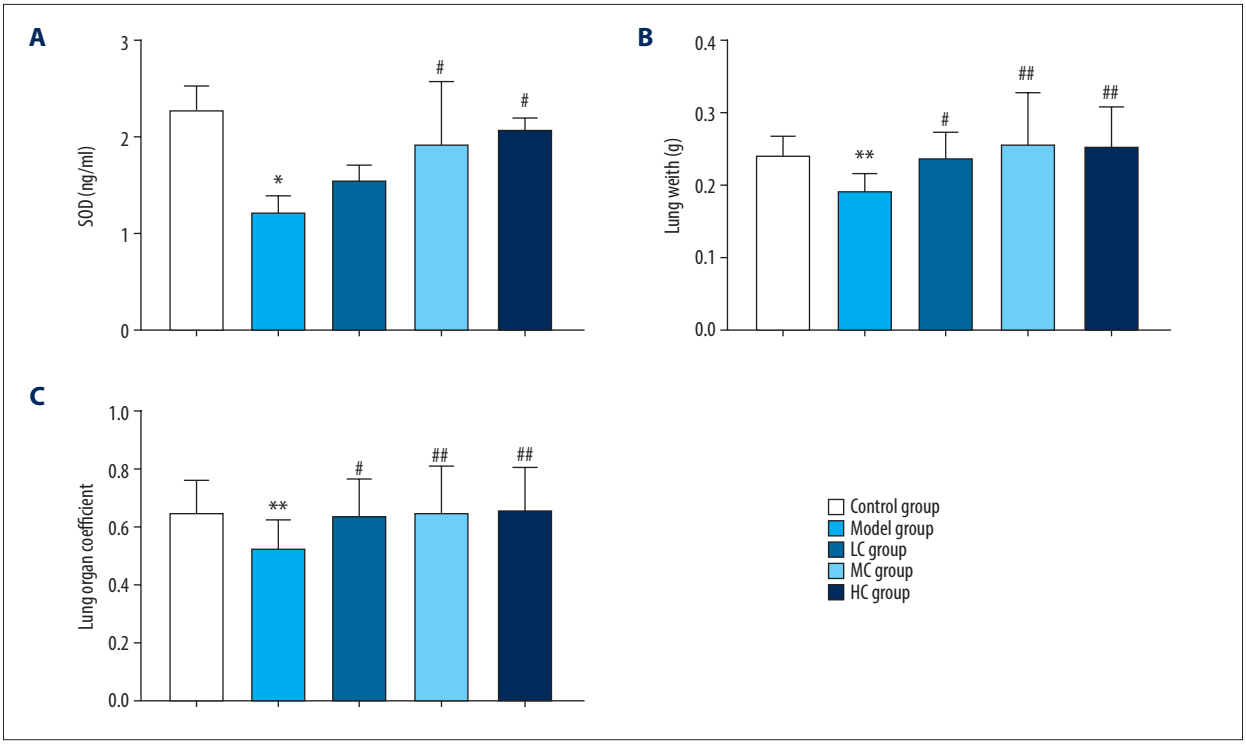

Figure 2. Determination of aging-related indexes. (**A**) SOD activity in each group. (**B**) Lung weight in each group. (**C**) Lung organ coefficient in each group. LC group: low-dose *Codonopsis pilosula* treatment group, MC group: middle-dose *Codonopsis pilosula* treatment group, HC group: high-dose *Codonopsis pilosula* treatment group. (Mean±SD, n=20, * $P<0.05$, ** $P<0.01$ *vs.* the control group, # $P<0.05$, ## $P<0.01$ *vs.* the model group).

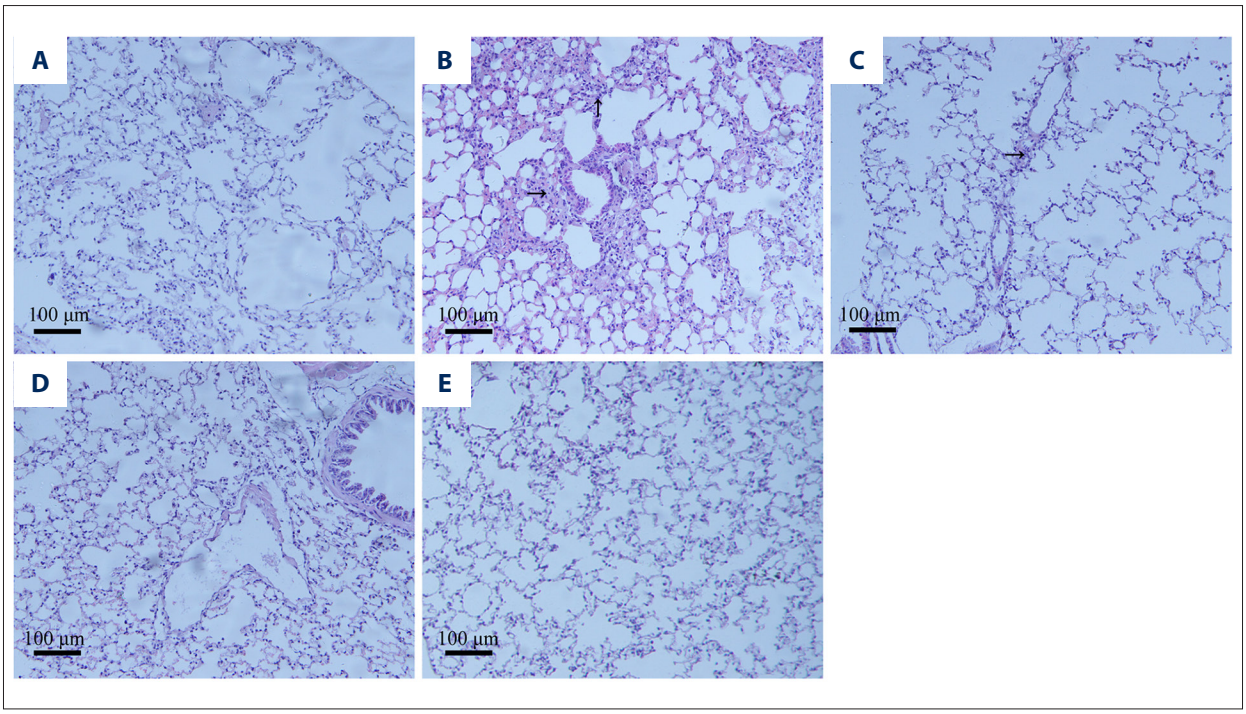

Figure 3. Pathological results of lung tissue in each group (HE×10). (**A**) The control group. (**B**) The model group. (**C**) Low-dose *Codonopsis pilosula* treatment group. (**D**) Middle-dose *Codonopsis pilosula* treatment group. (**E**) High-dose *Codonopsis pilosula* treatment group. Fibroblast (↑), extracellular matrix (→).

Indexed in: [Current Contents/Clinical Medicine] [SCI Expanded] [ISI Alerting System] [ISI Journals Master List] [Index Medicus/MEDLINE] [EMBASE/Excerpta Medica] [Chemical Abstracts/CAS]

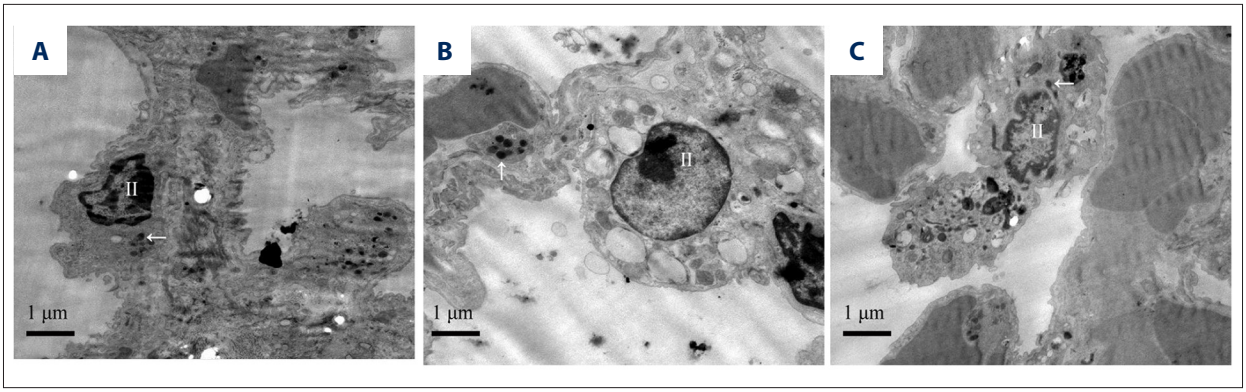

Figure 4. Transmission electron microscopic observation of the lung tissue (10 000×). (**A**) The control group. (**B**) The model group. (**C**) High-dose *Codonopsis pilosula* treatment group. Platelet (↑), type II alveolar epithelial cell (II), lamellar body (←).

Ultrastructural observation of lung tissue

In the control group, the main structures were the alveolar cavity and type II alveolar epithelial cells (Figure 4A). In the model group, platelets attached to the alveolar vascular cavity and many platelets gathered in capillaries. The lamellar bodies in type II alveolar epithelial cells completely exfoliated (Figure 4B). In the HC group, there were more type II alveolar epithelial cells and no significant changes in the alveolar cavity, lamellar bodies, and mitochondria (Figure 4C). These results suggest that *Codonopsis pilosula* improved the ultrastructure of lung tissue cells in aging mice.

Differentially expressed lncRNAs, mRNAs, and miRNAs in the model group compared with the control group and HC group compared with the model group

To identify differentially expressed lncRNAs, mRNAs, and miRNAs between groups, we performed microarray analysis. The expression levels of lncRNAs, mRNAs, and miRNAs in the control group, model group, and HC group were detected by microarray analysis. We found that 31879 lncRNAs, 28579 mRNAs, and 423 miRNAs were changed in the model group compared with the control group, and 31 427 lncRNAs, 27 418 mRNAs, and 461 miRNAs were dysregulated after high-dose *Codonopsis pilosula* treatment. lncRNAs, mRNAs, and miRNAs were significantly changed in the model group compared with the control group and HC group compared with the model group, with fold change $|FC| \geq 2$ and $P<0.05$. Compared with the control group, a total of 138 differentially expressed lncRNAs were identified, with 125 upregulated and 13 downregulated in the model group. A total of 128 mRNAs were identified, with 116 upregulated and 12 downregulated. A total of 7 differentially expressed miRNAs were identified, with 6 upregulated and 1 downregulated.

Compared with the model group, a total of 282 differentially expressed lncRNAs were identified, with 92 upregulated and 190 downregulated in the HC group. A total of 283 mRNAs were identified, with 58 upregulated and 225 downregulated. A total of 19 differentially expressed miRNAs were identified, with 13 upregulated and 6 downregulated. As shown in Figure 5A–5F, the volcano plots showed differentially expressed lncRNAs, mRNAs, and miRNAs between groups. The top 50 upregulated and downregulated lncRNAs, mRNAs, and miRNAs in the model group compared with the control group and HC group compared with the model group are listed in Supplementary Tables 1–3. Surprisingly, we found 73 common lncRNAs and 63 common mRNAs with different expressions between the HC group compared with the model group and the model group compared with the control group (Figure 5G, 5H, and Supplementary Table 4). There was no significant change in the expression levels of these genes in the HC group compared with the control group. These results indicate that treatment with *Codonopsis pilosula* can reverse the gene expression changes caused by aging.

Function enrichment analysis

GO enrichment analysis of differentially expressed mRNAs in the model group compared with the control group and HC group compared with the model group was conducted to assess their functions. Detoxification of copper ion, synapse, and copper ion binding were significantly enriched GO terms in the model group compared with the control group (Figure 6A). Amino acid transport, outer dense fiber, and amino acid transmembrane transporter activity were significantly enriched GO terms in the HC group compared with the model group (Figure 6B).

Then, KEGG pathway analysis of differentially expressed mRNAs was performed to explore the signaling pathways involved. The results showed that differentially expressed mRNAs in the model group compared with the control group were associated with 7 pathways, and differentially expressed mRNAs in the HC group compared with the model group were associated with 17 pathways. Calcium signaling pathway, mineral

Indexed in: [Current Contents/Clinical Medicine] [SCI Expanded] [ISI Alerting System] [ISI Journals Master List] [Index Medicus/MEDLINE] [EMBASE/Excerpta Medica] [Chemical Abstracts/CAS]

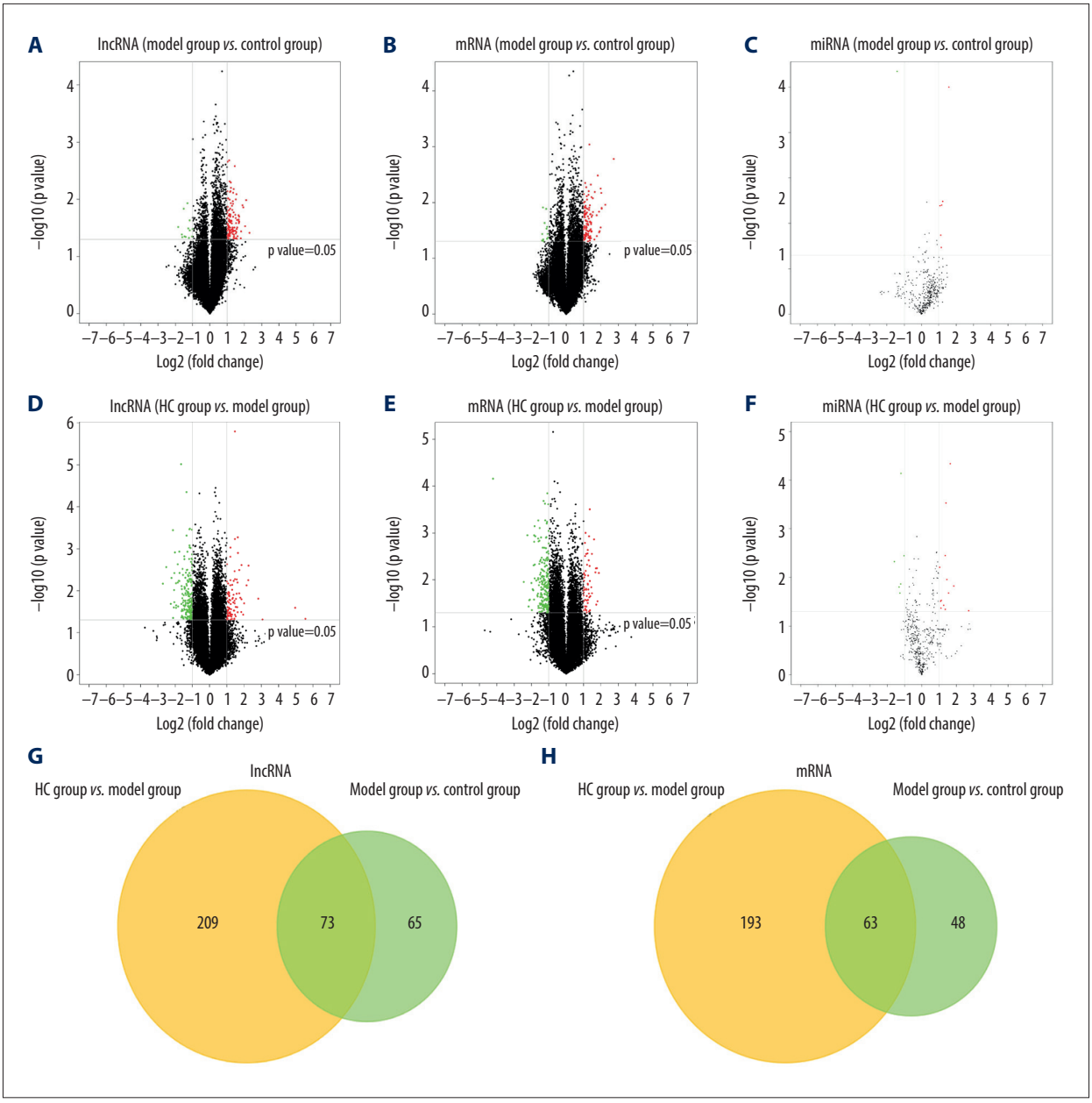

Figure 5. Volcano plots showing differentially expressed lncRNAs, mRNAs, and miRNAs between groups. (**A–F**) Volcano plot for differentially expressed lncRNA, mRNA, and miRNA in the model group compared with the control group and HC group compared with the model group. Upregulated genes are shown in red, the downregulated genes are shown in green, and the genes in black were not significantly different. Volcano plots directly reflect the number, significance, and reliability of differential genes. When the points in the diagram are closer to the upper left and the upper right, the difference is more significant. (**G, H**) Common lncRNAs and mRNAs with different expressions between the HC group compared with the model group and the model group compared with the control group. HC group: high-dose *Codonopsis pilosula* treatment group.

absorption, and drug metabolism-other enzymes were significantly enriched pathways in the model group compared with the control group (Figure 6C), and transcriptional misregulation in cancer, metabolic pathways, and cytokine-cytokine receptor interaction were significantly enriched pathways in the HC group compared with the model group (Figure 6D). Metabolic pathways were the common pathway between the model group compared with the control group and HC group compared with the model group.

Indexed in: [Current Contents/Clinical Medicine] [SCI Expanded] [ISI Alerting System] [ISI Journals Master List] [Index Medicus/MEDLINE] [EMBASE/Excerpta Medica] [Chemical Abstracts/CAS]

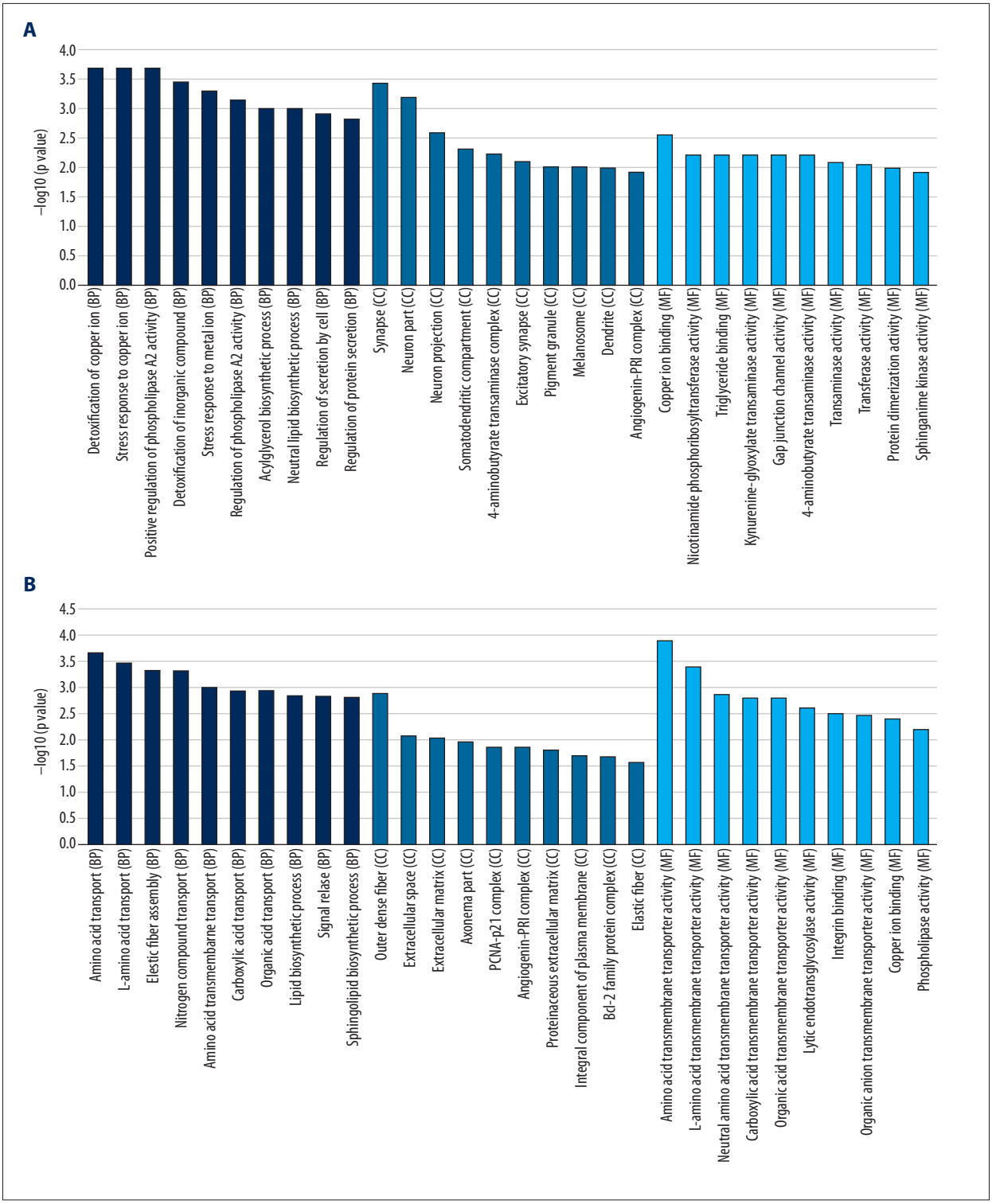

Indexed in: [Current Contents/Clinical Medicine] [SCI Expanded] [ISI Alerting System] [ISI Journals Master List] [Index Medicus/MEDLINE] [EMBASE/Excerpta Medica] [Chemical Abstracts/CAS]

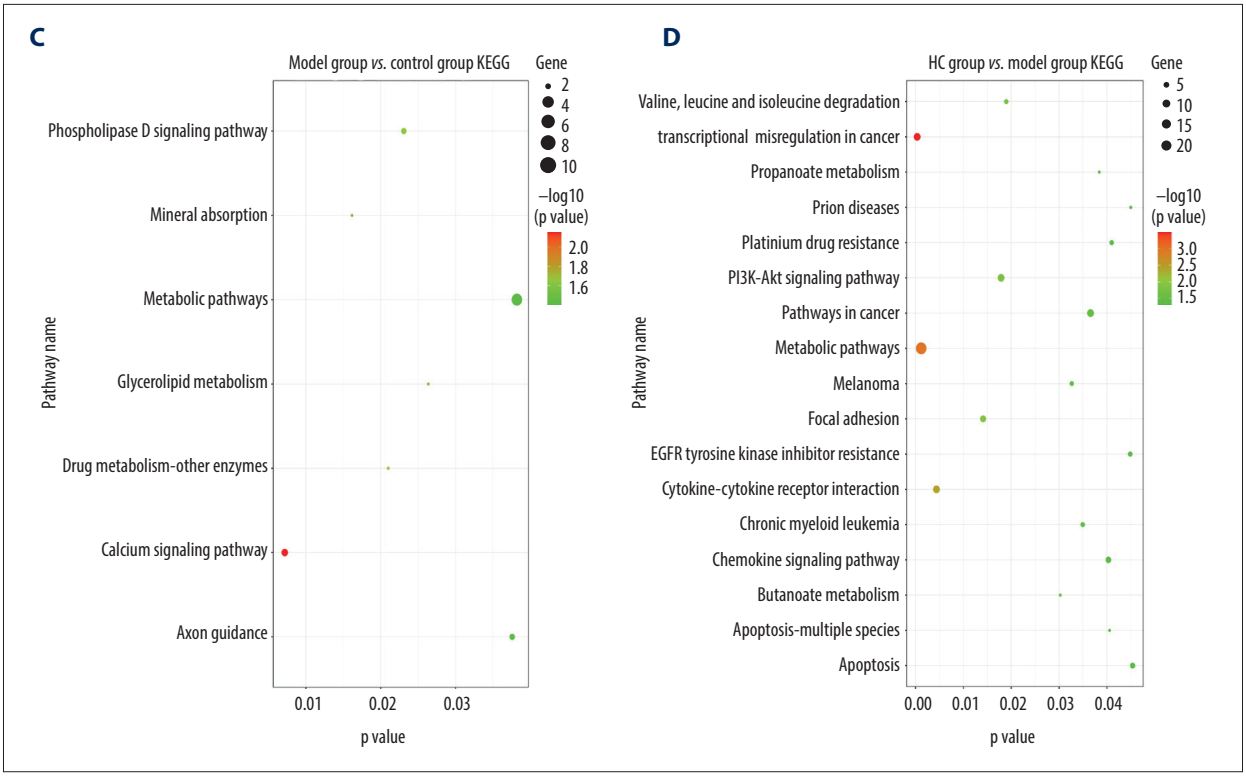

Figure 6. GO enrichment analysis and KEGG pathway analysis. (**A**) GO analysis of differentially expressed mRNAs in the model group compared with the control group, with the top 10 significantly enriched GO terms, including biological processes (BP), cellular components (CC) and molecular functions (MF). (**B**) GO analysis of differentially expressed mRNAs in the HC group compared with the model group, with the top 10 significantly enriched GO terms, including biological processes (BP), cellular components (CC) and molecular functions (MF). (**C**) KEGG pathway analysis in the model group compared with the control group. (**D**) KEGG pathway analysis in the HC group compared with the model group. HC group: high-dose *Codonopsis pilosula* treatment group.

lncRNA-miRNA and miRNA-mRNA network in aging mice and after treatment with *Codonopsis pilosula*

In aging mice, a total of 52 lncRNA-miRNA and 19 miRNA-mRNA co-expression pairs with P<0.05 and r<0 were identified. These lncRNA-miRNA co-expression pairs consisted of 50 lncRNAs (44 upregulated and 6 downregulated lncRNAs) and 6 miRNAs (5 upregulated and 1 downregulated miRNAs) (Figure 7). These miRNA-mRNA co-expression pairs consisted of 2 miRNAs (1 upregulated and 1 downregulated miRNAs) and 19 mRNAs (18 upregulated and 1 downregulated mRNAs) (Figure 8).

After treatment with *Codonopsis pilosula*, a total of 85 lncRNA-miRNA and 63 miRNA-mRNA co-expression pairs with P<0.05 and r<0 were identified. These lncRNA-miRNA co-expression pairs consisted of 56 lncRNAs (11 upregulated and 45 downregulated lncRNAs) and 16 miRNAs (11 upregulated and 5 downregulated miRNAs) (Figure 9). These miRNA-mRNA co-expression pairs consisted of 9 miRNAs (8 upregulated and 1 downregulated miRNAs) and 47 mRNAs (3 upregulated and 44 downregulated mRNAs) (Figure 10).

ceRNA network in aging mice and after treatment with *Codonopsis pilosula*

Finally, the ceRNA network was constructed based on the lncRNA-miRNA network and miRNA-mRNA network. In aging mice, the ceRNA network consisted of 47 lncRNAs, with 44 upregulated and 3 downregulated, 2 miRNAs, with 1 upregulated and 1 downregulated, and 19 mRNAs, with 18 upregulated and 1 downregulated (Figure 11). After treatment with *Codonopsis pilosula*, there were 43 lncRNAs, with 3 upregulated and 40 downregulated, 8 miRNAs, with 7 upregulated and 1 downregulated, and 45 mRNAs, with 3 upregulated and 42 downregulated in the ceRNA network (Figure 12).

Compared with the ceRNA network in aging mice and after treatment with *Codonopsis pilosula*, we found 7 common mRNAs and 6 common lncRNAs. Hif3a, Zbtb16, Plxna2, Tfec, Tcf23, Mcf2l, and Tspan11 were upregulated in aging mice. NONMMUT063872, gi|755473727|ref|XR_400701.2|, gi|755474789|ref|XR_887412.1|, ri|D330026F23|PX00192L03|3026, and gi|755567664|ref|XR_882416.1| were upregulated

Indexed in: [Current Contents/Clinical Medicine] [SCI Expanded] [ISI Alerting System] [ISI Journals Master List] [Index Medicus/MEDLINE] [EMBASE/Excerpta Medica] [Chemical Abstracts/CAS]

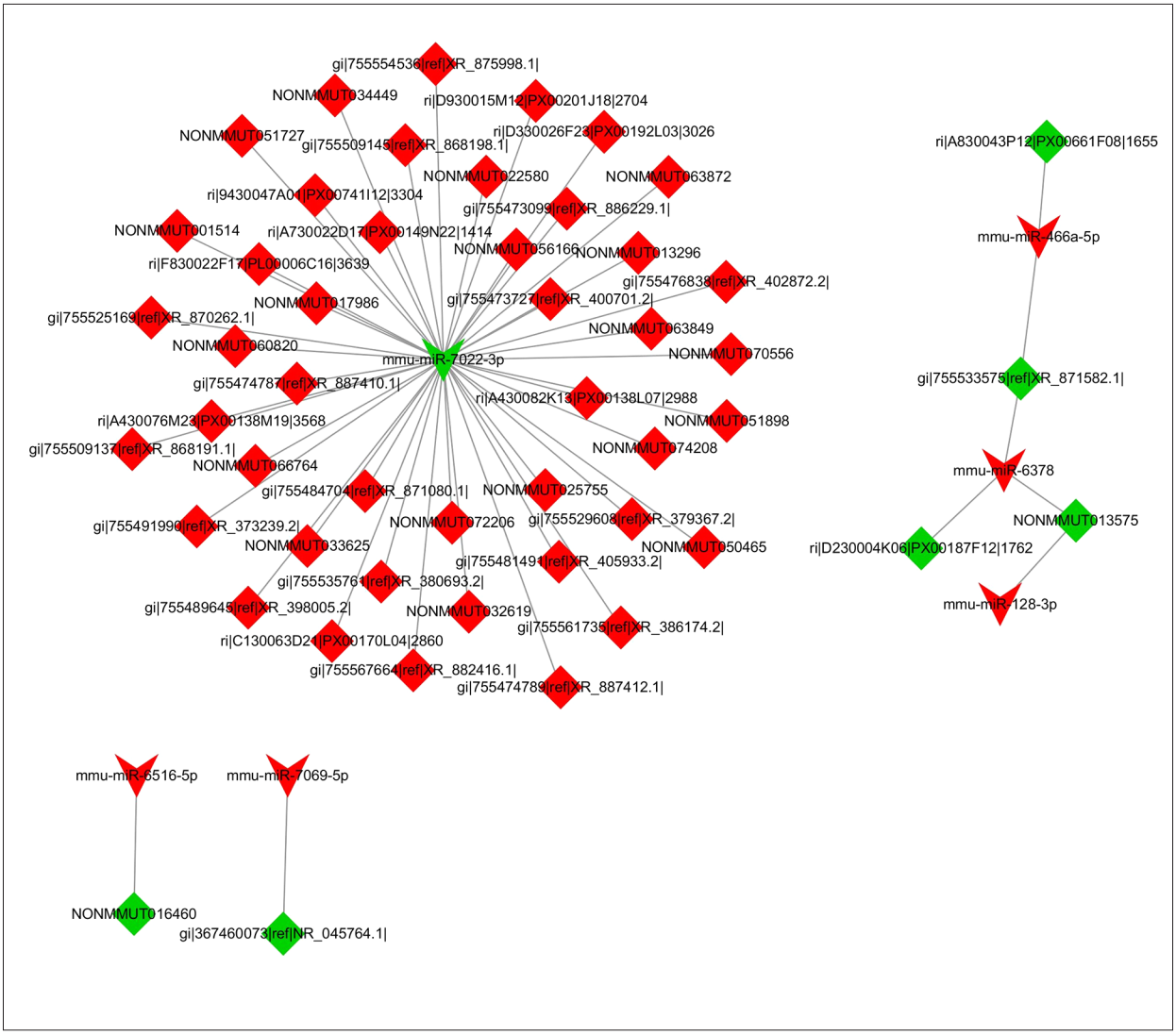

Figure 7. The differentially expressed lncRNA-miRNA network in aging mice. (The diamond and V shape represent lncRNA and miRNA, respectively. The red nodes indicate upregulation in the array data and the green nodes indicate downregulation in the array data.)

and ri|D230004K06|PX00187F12|1762 was downregulated in aging mice. However, the expression levels of these genes were reversed after treatment with *Codonopsis pilosula*, indicating that these genes are the genes involved in the anti-aging effect of *Codonopsis pilosula*.

Quantitative real-time polymerase chain reaction (qRT-PCR)

Compared with the ceRNA network in aging mice and after treatment with *Codonopsis pilosula*, we found 7 common mRNAs and 6 common lncRNAs. According to the degree value of the network node and the fold change of the microarray analysis, 3 mRNAs (Hif3a, Zbtb16, and Plxna2) and 1 lncRNA (NONMMUT063872) were examined using qRT-PCR. In accordance with the data from the microarray analysis, Hif3a, Zbtb16, and Plxna2 were upregulated in the model group compared with the control group and were downregulated in the HC group compared with the model group (Figure 13A–13C). NONMMUT063872 was significantly increased in the model group compared with the control group and was significantly decreased in the HC group compared with the model group (Figure 13D).

Discussion

Codonopsis pilosula is a traditional tonifying medicine that has many anti-aging effects. Research on the mechanism underlying the anti-aging effects of *Codonopsis pilosula* has mainly

Indexed in: [Current Contents/Clinical Medicine] [SCI Expanded] [ISI Alerting System] [ISI Journals Master List] [Index Medicus/MEDLINE] [EMBASE/Excerpta Medica] [Chemical Abstracts/CAS]

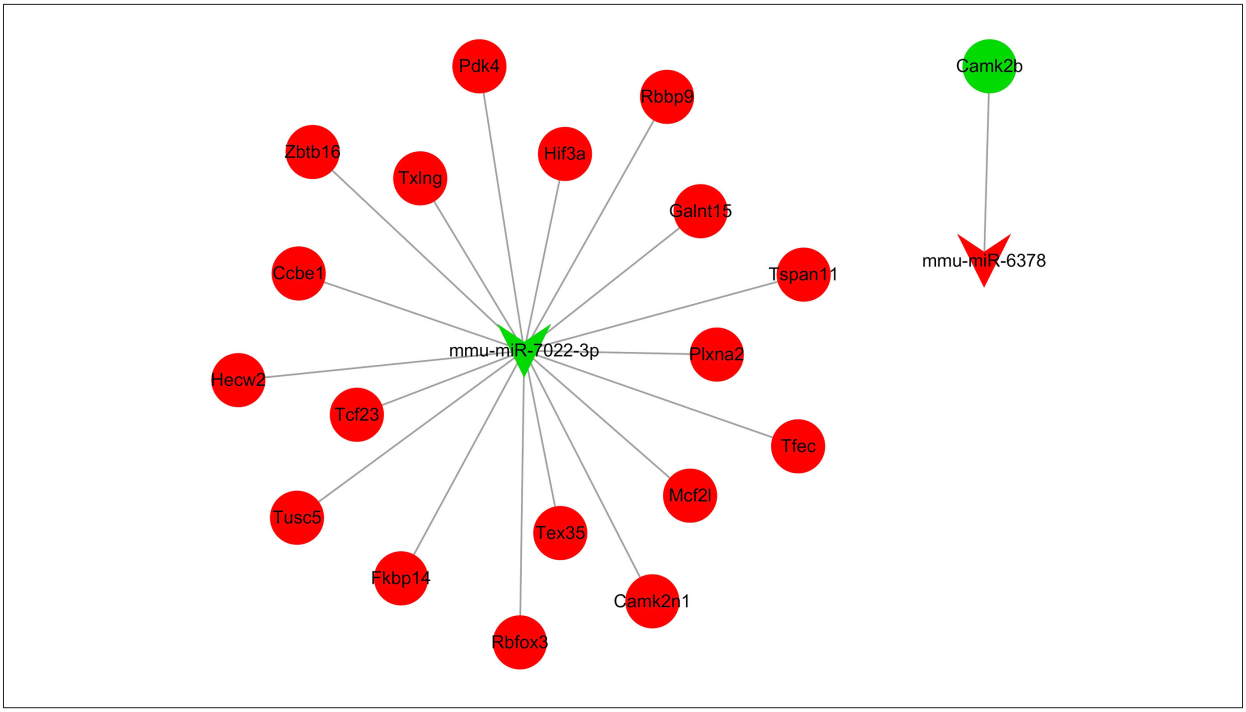

Figure 8. The differentially expressed miRNA-mRNA network in aging mice. (V shape and circle represent miRNA and mRNA, respectively. The red nodes indicate upregulation in the array data and the green nodes indicate downregulation in the array data.)

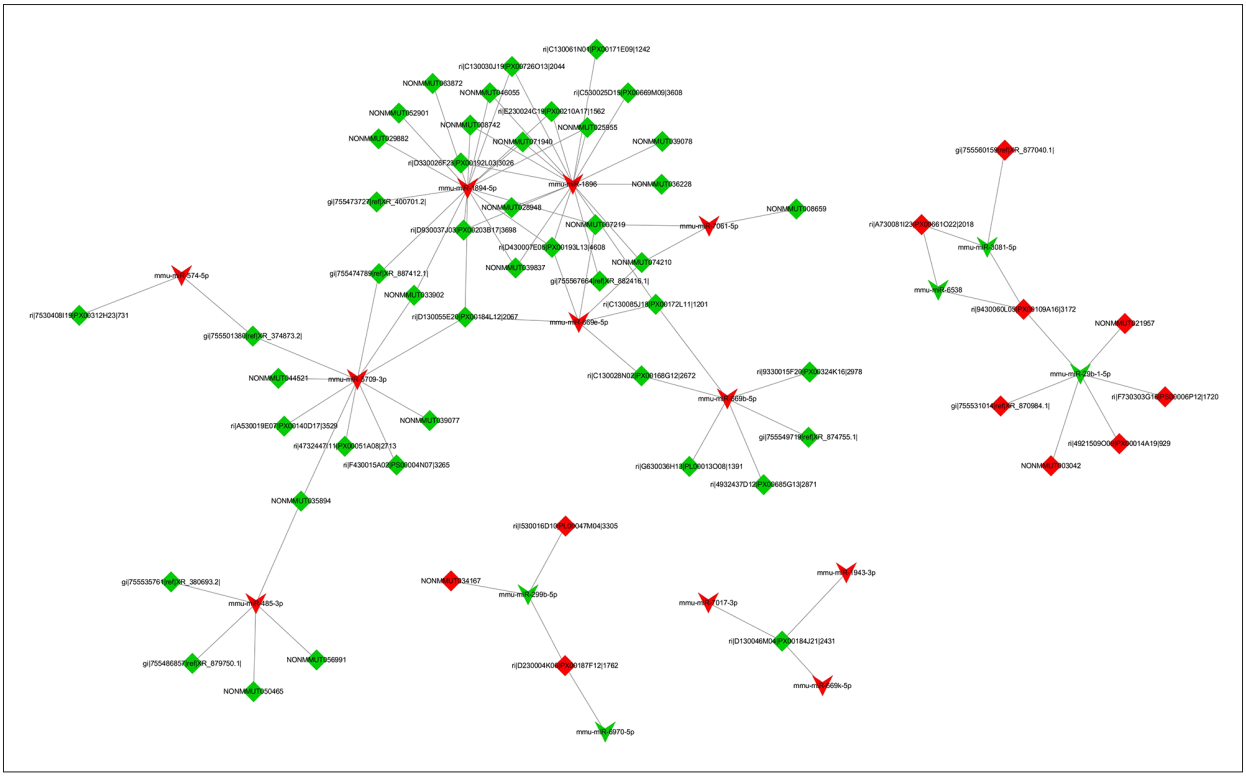

Figure 9. The differentially expressed lncRNA-miRNA network after treatment with *Codonopsis pilosula*. (The diamond and V shape represent lncRNA and miRNA, respectively. The red nodes indicate upregulation in the array data; the green nodes indicate downregulation in the array data.)

Indexed in: [Current Contents/Clinical Medicine] [SCI Expanded] [ISI Alerting System] [ISI Journals Master List] [Index Medicus/MEDLINE] [EMBASE/Excerpta Medica] [Chemical Abstracts/CAS]

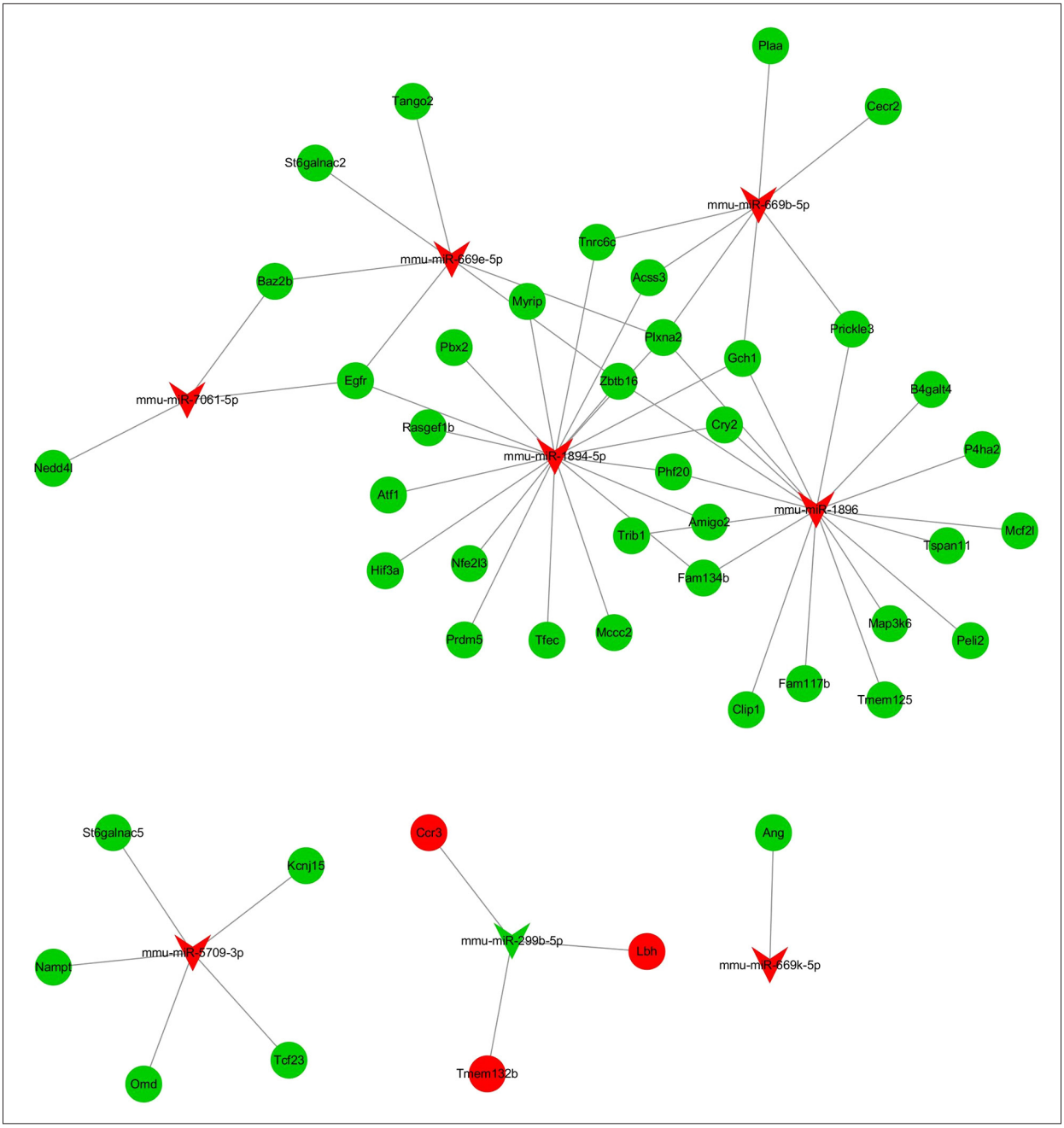

Figure 10. The differentially expressed miRNA-mRNA network after treatment with *Codonopsis pilosula*. (V shape and circle represent miRNA and mRNA, respectively. The red nodes indicate upregulation in the array data and the green nodes indicate downregulation in the array data.)

focused on scavenging free radicals and anti-oxidation [13]; inhibiting nerve cell apoptosis [14]; significantly increasing the thymus and spleen index of D-galactose-induced aging mice, delaying the aging of immune organs, and enhancing immune function [15]. In the present study, an aging mouse model was established followed by treatment with *Codonopsis pilosula*. Our results showed that we successfully established the aging model, and *Codonopsis pilosula* protected the lungs of aging mice. To explore the molecular mechanism underlying the anti-aging effect of *Codonopsis pilosula*, we performed microarray analysis to assess the expression levels of lncRNAs, mRNAs, and miRNAs in the control group, model group, and HC group. We obtained differentially expressed lncRNAs, mRNAs, and miRNAs between groups and constructed the ceRNA network in aging mice and after treatment with *Codonopsis pilosula*. Compared with the ceRNA network in aging mice and

Indexed in: [Current Contents/Clinical Medicine] [SCI Expanded] [ISI Alerting System] [ISI Journals Master List] [Index Medicus/MEDLINE] [EMBASE/Excerpta Medica] [Chemical Abstracts/CAS]

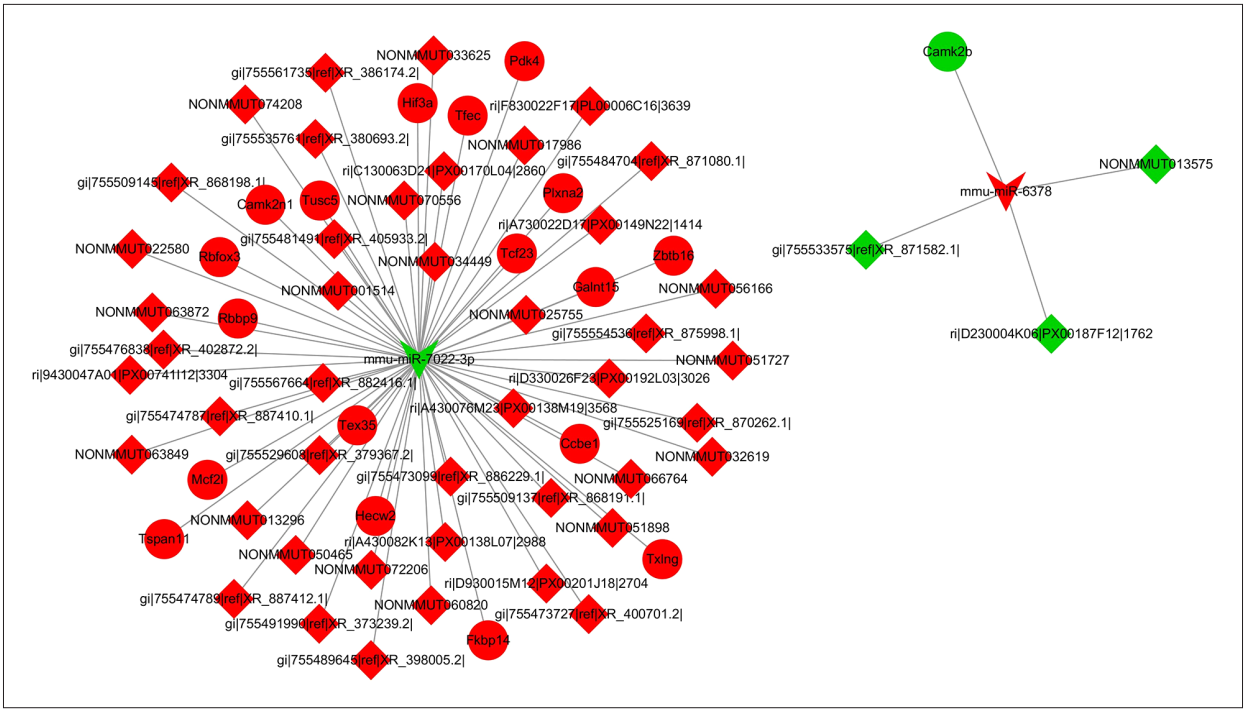

Figure 11. The differentially expressed ceRNA network in aging mice. (The diamond, V shape, and circle represent the lncRNA, miRNA, and mRNA, respectively. The red nodes indicate upregulation in the array data and the green nodes indicate downregulation in the array data.)

after treatment with *Codonopsis pilosula*, we found 3 mRNAs (Hif3a, Zbtb16, and Plxna2) and 1 lncRNA (NONMMUT063872) that were associated with the anti-aging effect of *Codonopsis pilosula* and they were validated by qRT-PCR. Our results suggest that the ceRNA network plays an important role in the anti-aging effect of *Codonopsis pilosula*.

SOD is a very important antioxidant defense against oxidative stress in the body. SOD is considered an anti-aging enzyme, and the level of natural SOD in the body decreases with age [16]. Studies showed that aging mice exhibited significant organ atrophy and reduced organ coefficient [17,18]. As shown in Figure 2, we found that SOD activity, lung weights, and lung organ coefficients of aging mice were significantly lower compared with the control group, which is consistent with previous reports. After treatment with *Codonopsis pilosula*, SOD activity, lung weights, and lung organ coefficients were significantly increased. Our results showed that we successfully established the aging model, and *Codonopsis pilosula* had a protective effect on the lungs of aging mice.

In our experiments, the protective effect of *Codonopsis pilosula* on the lungs of aging mice was also demonstrated in both histology and ultrastructure. To observe the pathological changes in lung tissue, we performed HE staining. Fibroblasts are involved in tissue repair and extracellular matrix remodeling [19]. Most aging-related lung diseases exhibit extracellular matrix remodeling [20]. These facts suggest that fibroblasts proliferation and extracellular matrix aggregation are associated with aging-related lung diseases, which is consistent with our results (Figure 3B). After treatment with *Codonopsis pilosula*, the pathology of lung tissue of aging mice was improved. These results suggested that *Codonopsis pilosula* can improve the pathology of lung tissue in aging mice. To observe the ultrastructural changes of lung tissue cells, we performed transmission electron microscopy. Studies have shown that increased platelet activity is associated with aging, and with platelet overreaction in older adults and aging mice, resulting in thrombosis [21,22]. Bone marrow compartments analysis showed that platelet bias hematopoiesis plays an important role in aging mice, as reflected by thrombocytosis [21]. As shown in Figure 4B, platelets attached to the alveolar vascular cavity, and many platelets gathered in capillaries in the model group, which is consistent with previous reports. Type II alveolar epithelial cells have an important role to maintaining the integrity of normal lung structure, and dysfunction of these cells is very important in a variety of respiratory diseases [23]. Their main function is to synthesize and secrete surface-active substances [24]. In type II alveolar epithelial cells, lamellar bodies are the sites for pulmonary surfactant synthesis, storage, and secretion [25]. Shedding of lamellar bodies affects the function of type II alveolar epithelial cells and can lead to a variety of respiratory diseases. In the present study, the lamellar bodies in type II alveolar epithelial cells

Indexed in: [Current Contents/Clinical Medicine] [SCI Expanded] [ISI Alerting System] [ISI Journals Master List] [Index Medicus/MEDLINE] [EMBASE/Excerpta Medica] [Chemical Abstracts/CAS]

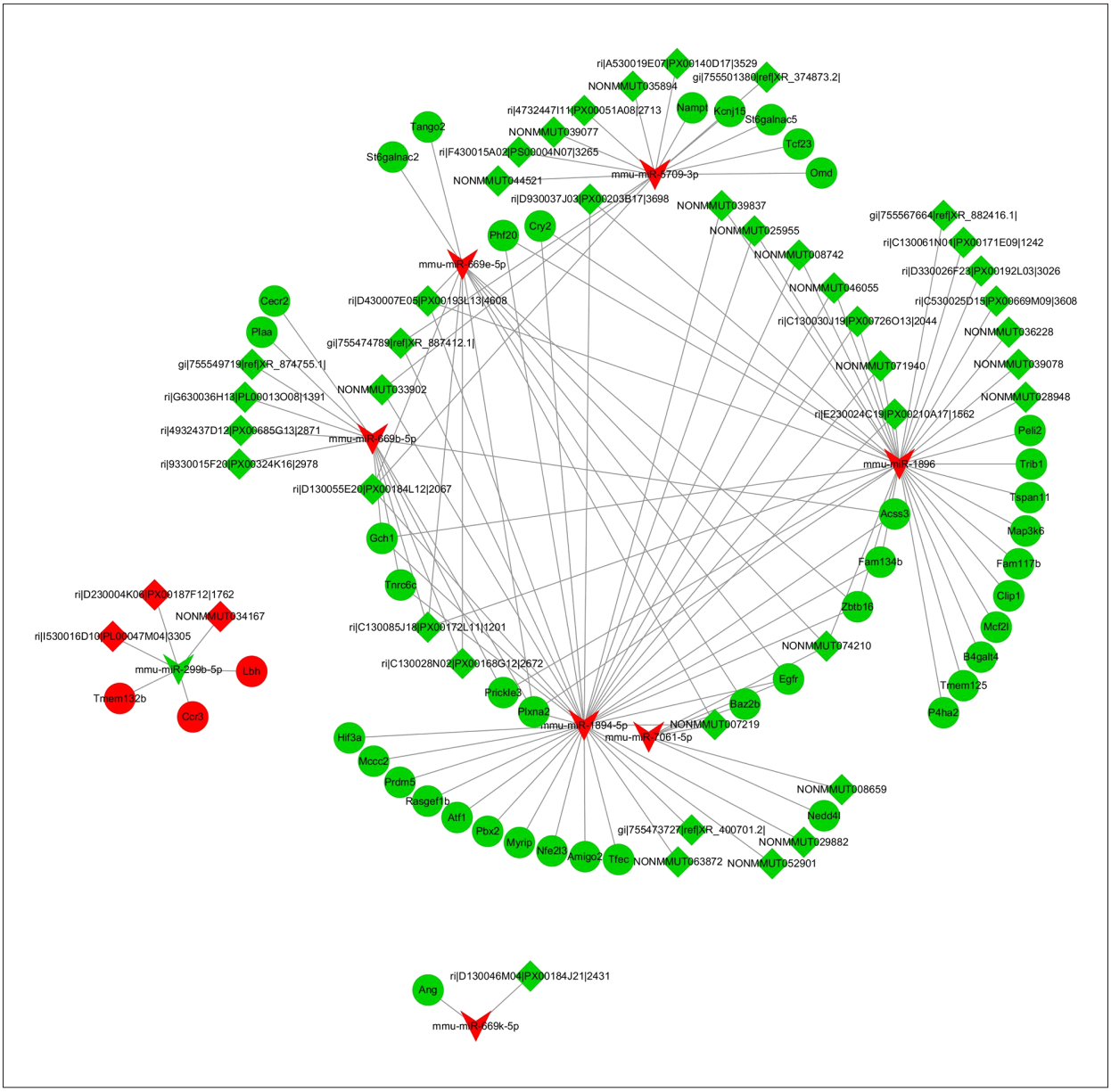

Figure 12. The differentially expressed ceRNA network after treatment with *Codonopsis pilosula*. (The diamond, V shape, and circle represent lncRNA, miRNA, and mRNA, respectively. The red nodes indicate upregulation in the array data and the green nodes indicate downregulation in the array data.)

were completely exfoliated (Figure 4B), suggesting that aging increases susceptibility to respiratory diseases. However, in the HC group, there were more type II alveolar epithelial cells and no significant changes in the alveolar cavity, lamellar bodies, and mitochondria (Figure 4C). These results suggest that *Codonopsis pilosula* can improve the ultrastructure of lung tissue cells in aging mice.

We also performed lncRNA, mRNA, and miRNA microarray analysis in the control group, model group, and HC group to study the molecular mechanism underlying the anti-aging effect of *Codonopsis pilosula*. Microarray analysis showed that 138 lncRNAs, 128 mRNAs, and 7 miRNAs were differentially expressed in the model group compared with the control group, whereas 282 lncRNAs, 283 mRNAs, and 19 miRNAs were differentially expressed in the HC group compared with the model group. After treatment with *Codonopsis pilosula*, amino acid transport, outer dense fiber, and amino acid transmembrane transporter activity were significantly enriched GO terms. KEGG pathway analysis of the differentially expressed genes also revealed some important pathways significantly related to aging, including butanoate metabolism, propanoate metabolism,

Indexed in: [Current Contents/Clinical Medicine] [SCI Expanded] [ISI Alerting System] [ISI Journals Master List] [Index Medicus/MEDLINE] [EMBASE/Excerpta Medica] [Chemical Abstracts/CAS]

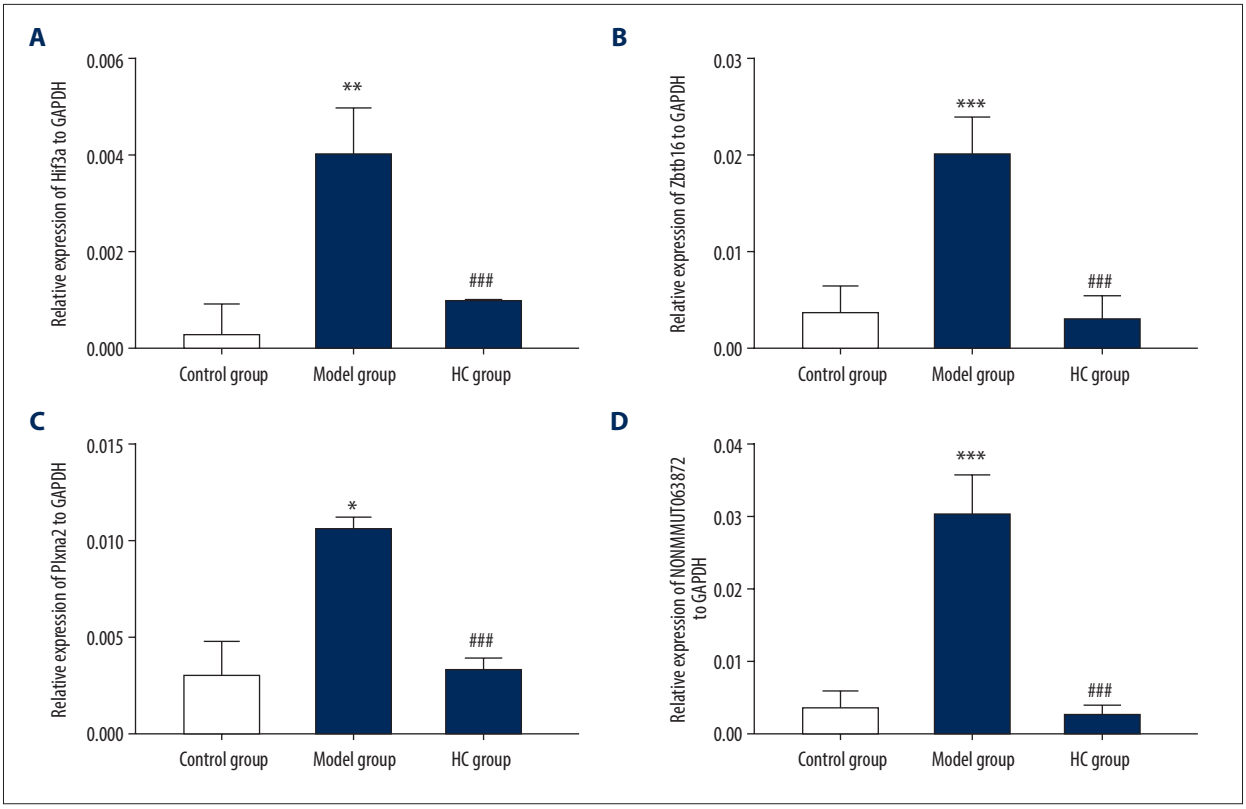

Figure 13. qRT-PCR verification of the gene expressions. (**A–C**) The expressions of Hif3a, Plxna2, and Zbtb16 were detected by qRT-PCR. (**D**) The expression of NONMMUT063872 was detected by qRT-PCR. HC group: high-dose *Codonopsis pilosula* treatment group. (Mean±SD, n=3, * $P<0.05$, ** $P<0.01$, *** $P<0.001$ *vs.* the control group, ### $P<0.001$ *vs.* the model group).

metabolic pathway, and PI3K-Akt signaling pathway. The PI3K-Akt signaling pathway has previously been reported to be associated with aging [26]. Studies have shown that an increased metabolic rate can delay aging [27]. Butanoate metabolism, propanoate metabolism, and metabolic pathway are known to be involved in metabolism, which suggests that they might be involved in the anti-aging effect of *Codonopsis pilosula*.

In this study, we constructed the ceRNA network in aging mice and after treatment with *Codonopsis pilosula* based on lncRNA-miRNA and miRNA-mRNA co-expression networks. Compared with the ceRNA network in aging mice and after treatment with *Codonopsis pilosula*, we found 7 common mRNAs and 6 common lncRNAs, indicating that these genes may be associated with the anti-aging effect of *Codonopsis pilosula*. Then, 3 mRNAs (Hif3a, Zbtb16, and Plxna2) and 1 lncRNA (NONMMUT063872) among the common genes were verified using qRT-PCR. The results were consistent with the microarray analysis, proving the reliability of the microarray results. Hypoxia-inducible factors (HIF) are heterodimeric transcription factors that allow cells to adapt and survive during hypoxia, and the expression of HIF3A is increased during hypoxia [28]. Aging is correlated with a reduction of cellular oxygen supply, which is characterized by decreased oxygen supply to tissue, a reduction of tissue PO2, and the activity of several enzymes and metabolic factors [29]. Hif3a (hypoxia-inducible factor 3A gene) has been reported to show significant differences in elderly tissues and is positively correlated with aging [30]. In the present study, we found that Hif3a was significantly upregulated in the model group. However, the expression level was significantly downregulated after treatment with *Codonopsis pilosula*, providing evidence of the protective effect of *Codonopsis pilosula* in the lungs of aging mice. HIF-3α plays an important negative regulatory role in enhancing the physical endurance of rats [31]. A variety of splicing variants of HIF-3α are encoded by gene HIF3A [32]; therefore, decreased expression of HIF3A can enhance endurance. After treatment with *Codonopsis pilosula*, HIF3A was significantly downregulated, indicating that *Codonopsis pilosula* enhanced endurance and had an anti-fatigue effect. The actual aging of the lungs occurs in the resident cells and is closely related to aging of the immune system (immune aging) [19]. ZBTB16 (Zinc Finger and BTB Domain Containing 16) is a transcription factor involved in the regulation of diverse biological processes, including cell proliferation, differentiation, stem cell maintenance, organ development, and innate immune cell development [33], indicating that ZBTB16 may be associated with lung aging. Plxna2 is a known molecule that regulates axonal guidance in nerve development [34]

Indexed in: [Current Contents/Clinical Medicine] [SCI Expanded] [ISI Alerting System] [ISI Journals Master List] [Index Medicus/MEDLINE] [EMBASE/Excerpta Medica] [Chemical Abstracts/CAS]

and it is also related to lung development [35]. In the present study, we found this gene is regulated in the lungs during aging and the gene expression was reversed after treatment with *Codonopsis pilosula*.

A high degree of enrichment means that enrichment plays an important role [36] in the anti-aging effect of *Codonopsis pilosula*. In the ceRNA network after treatment with *Codonopsis pilosula*, miR-1894-5p was the most significantly upregulated miRNA and was associated with 36 enriched genes, while Plxna2 was the most significantly downregulated mRNA and was associated with 4 enriched genes. Notably, lncRNA NONMMUT063872 competed for combining with miR-1894-5p and then affected the expression of Plxna2. Our results showed that NONMMUT063872 decreased, miR-1894-5p increased, and Plxna2 decreased after treatment with *Codonopsis pilosula*. Because Plxna2 is the target of miR-1894-5p, further study is needed of the mechanisms underlying the anti-aging effect of lncRNA NONMMUT063872 in *Codonopsis pilosula*.

Conclusions

Our results show that treatment with *Codonopsis pilosula* can improve the pathological and cellular ultrastructural changes of lung tissue in aging mice. Through microarray analysis and bioinformatics methods, we constructed the ceRNA network in aging mice and after treatment with *Codonopsis pilosula*. Compared with the ceRNA network in aging mice without and with treatment with *Codonopsis pilosula*, several hub genes (Hif3a, Zbtb16, Plxna2, and NONMMUT063872) were found and verified using qRT-PCR. Our results showed that these RNAs and the network they are involved in may contribute to the anti-aging effect of *Codonopsis pilosula*.

Acknowledgements

We thank Junjun Liu for help with animal experiments and Chunhua Wang for histopathological analysis.

Conflicts of interest

None.

Supplementary Data

Supplementary Table 1. The top 50 upregulated and downregulated lncRNAs in the model group compared with the control group and the HC group compared with the model group.

Supplementary Table 2. The top 50 upregulated and downregulated mRNAs in the model group compared with the control group and the HC group compared with the model group.

Supplementary/raw data available from the corresponding author on request.

Supplementary Table 3. The top 50 upregulated and downregulated miRNAs in the model group compared with the control group and the HC group compared with the model group.

Supplementary Table 4. Common lncRNAs and mRNAs with different expressions between the HC group compared with the model group and the model group compared with the control group.

References:

1. Xia X, Chen W, McDermott J, Han JJ: Molecular and phenotypic biomarkers of aging. F1000Res, 2017; 6: 860
2. Lara J, Sherratt MJ, Rees M: Aging and anti-aging. Maturitas, 2016; 93: 1–3
3. Skloot GS: The effects of aging on lung structure and function. Clin Geriatr Med, 2017; 33: 447–57
4. Hecker L: Mechanisms and consequences of oxidative stress in lung disease: Therapeutic implications for an aging populace. Am J Physiol Lung Cell Mol Physiol, 2018; 314: L642–53
5. Gao SM, Liu JS, Wang M et al: Traditional uses, phytochemistry, pharmacology and toxicology of Codonopsis: A review. J Ethnopharmacol, 2018; 219: 50–70
6. Cai J, Ashraf MA, Luo L, Tang H: Effects of *Codonopsis pilosula* water extract on MicroRNA expression profile in D-galactose-induced senile mice. Pak J Pharm Sci, 2017; 30: 1179–83
7. Zhan G, Yang N, Xiao B: [Rich selenium-banqiao-*Codonopsis pilosula* mixture enhances immune function of aging mice]. Xi Bao Yu Fen Zi Mian Yi Xue Za Zhi, 2015; 31: 1346–49 [in Chinese]
8. Salmena L, Poliseno L, Tay Y et al: A ceRNA hypothesis: The Rosetta Stone of a hidden RNA language? Cell, 2011; 146: 353–58
9. Li J, Wu Z, Zheng D et al: Bioinformatics analysis of the regulatory lncRNA-miRNA-mRNA network and drug prediction in patients with hypertrophic cardiomyopathy. Mol Med Rep, 2019; 20: 549–58
10. Gao Z, Fu P, Yu Z et al: Comprehensive analysis of lncRNA-miRNA- mRNA network ascertains prognostic factors in patients with colon cancer. Technol Cancer Res Treat, 2019; 18: 1533033819853237
11. Chen K, Ma Y, Wu S et al: Construction and analysis of a lncRNA-miRNA-mRNA network based on competitive endogenous RNA reveals functional lncRNAs in diabetic cardiomyopathy. Mol Med Rep, 2019; 20: 1393–403
12. Guo YN, Luo B, Chen WJ et al: Comprehensive clinical implications of homeobox A10 in 3,199 cases of non-small cell lung cancer tissue samples combining qRT-PCR, RNA sequencing and microarray data. Am J Transl Res, 2019; 11: 45–66
13. Geng GQ, Li NL, Liu H et al: [Effects of aqueous extract of *Codonopsis pilosula* on DNA and tissue structure of liver and kidney cells of aging mice induced by D-galactose]. Zhong Yi Yan Jiu, 2015; 28: 63–66 [in Chinese]

Indexed in: [Current Contents/Clinical Medicine] [SCI Expanded] [ISI Alerting System] [ISI Journals Master List] [Index Medicus/MEDLINE] [EMBASE/Excerpta Medica] [Chemical Abstracts/CAS]

14. Zhang F, Wang L, Che M, Wang Y: [Effects of aqueous extract of *Codonopsis pilosula* on brain cell apoptosis and related gene expression in aging model mice]. Zhong Guo Lao Nian Xue Za Zhi, 2010; 30: 2807–9 [in Chinese]
15. Zhang P, Hu LH, Bai RB et al: Structural characterization of a pectic polysaccharide from *Codonopsis pilosula* and its immunomodulatory activities *in vivo* and *in vitro*. Int J Biol Macromol, 2017; 104: 1359–69
16. Younus H: Therapeutic potentials of superoxide dismutase. Int J Health Sci (Qassim), 2018; 12: 88–93
17. Du HM, Wang YJ, Liu X et al: Defective central immune tolerance induced by high-dose D-galactose resembles aging. Biochemistry Mosc, 2019; 84: 617–26
18. Chen P, Chen F, Zhou B: Antioxidative, anti-inflammatory and anti-apoptotic effects of ellagic acid in liver and brain of rats treated by D-galactose. Sci Rep, 2018; 8: 1465
19. Brandenberger C, Muhlfeld C: Mechanisms of lung aging. Cell Tissue Res, 2017; 367: 469–80
20. Meiners S, Eickelberg O, Königshoff M: Hallmarks of the ageing lung. Eur Respir J, 2015; 45: 807–27
21. Davizon-Castillo P, McMahon B, Aguila S et al: TNF-alpha driven inflammation and mitochondrial dysfunction define the platelet hyperreactivity of aging. Blood, 2019; 134: 727–40
22. Montenont E, Rondina MT, Campbell RA: Altered functions of platelets during aging. Curr Opin Hematol, 2019; 26: 336–42
23. Shiraishi K, Nakajima T, Shichino S: *In vitro* expansion of endogenous human alveolar epithelial type II cells in fibroblast-free spheroid culture. Biochem Biophys Res Commun, 2019; 515: 579–85
24. Tian Y, Li Y, Li J et al: Bufei Yishen granule combined with acupoint sticking improves pulmonary function and morphormetry in chronic obstructive pulmonary disease rats. BMC Complement Altern Med, 2015; 15: 266
25. Haller T, Cerrada A, Pfaller K et al: Polarized light microscopy reveals physiological and drug-induced changes in surfactant membrane assembly in alveolar type II pneumocytes. Biochim Biophys Acta Biomembr, 2018; 1860: 1152–61
26. Zhang Y, Liu B, Chen X et al: Naringenin ameliorates behavioral dysfunction and neurological deficits in a d-galactose-induced aging mouse model through activation of PI3K/Akt/Nrf2 pathway. Rejuvenation Res, 2017; 20: 462–72
27. Azzu V, Valencak TG: Energy metabolism and ageing in the mouse: A mini-review. Gerontology, 2017; 63: 327–36
28. Janaszak-Jasiecka A, Bartoszewska S, Kochan K et al: miR-429 regulates the transition between hypoxia-inducible factor (HIF)1A and HIF3A expression in human endothelial cells. Sci Rep, 2016; 6: 22775
29. Cataldi A, Di Giulio C: "Oxygen supply" as modulator of aging processes: Hypoxia and hyperoxia models for aging studies. Curr Aging Sci, 2009; 2: 95–102
30. Ebersole JL, Novak MJ, Orraca L et al: Hypoxia-inducible transcription factors, HIF1A and HIF2A, increase in aging mucosal tissues. Immunology, 2018; 154: 452–64
31. Drevytska T, Gavenauskas B, Drozdovska S et al: HIF-3α mRNA expression changes in different tissues and their role in adaptation to intermittent hypoxia and physical exercise. Pathophysiology, 2012; 19: 205–14
32. Pasanen A, Heikkilä M, Rautavuoma K et al: Hypoxia-inducible factor (HIF)-3alpha is subject to extensive alternative splicing in human tissues and cancer cells and is regulated by HIF-1 but not HIF-2. Int J Biochem Cell Biol, 2010; 42: 1189–200
33. Jin Y, Nenseth HZ, Saatcioglu F: Role of PLZF as a tumor suppressor in prostate cancer. Oncotarget, 2017; 8: 71317–24
34. Oh JE, Kim HJ, Kim WS et al: PlexinA2 mediates osteoblast differentiation via regulation of Runx2. J Bone Miner Res, 2012; 27: 552–62
35. Perälä NM, Immonen T, Sariola H: The expression of plexins during mouse embryogenesis. Gene Expr Patterns, 2005; 5: 355–62
36. Hou Q, Huang Y, Liu Y et al: Profiling the miRNA-mRNA-lncRNA interaction network in MSC osteoblast differentiation induced by (+)-cholesten-3-one. BMC Genomics, 2018; 19: 783

Indexed in: [Current Contents/Clinical Medicine] [SCI Expanded] [ISI Alerting System] [ISI Journals Master List] [Index Medicus/MEDLINE] [EMBASE/Excerpta Medica] [Chemical Abstracts/CAS]